Title

Extracellular Matrix Hydrogel Promotes Tissue Remodeling, Arteriogenesis, and Perfusion in a Rat Hindlimb Ischemia Model.

Journal

JACC. Basic to translational science, 1(1-2)

ISSN

2452-302X

Authors

Ungerleider, Jessica L
Johnson, Todd D
Hernandez, Melissa J
et al.

Publication Date

2016

DOI

10.1016/j.jacbts.2016.01.009

Peer reviewed

JACC: BASIC TO TRANSLATIONAL SCIENCE
VOL. 1, NO. 1-2, 2016
ISSN 2452-302X
http://dx.doi.org/10.1016/j.jacbts.2016.01.009

PRE-CLINICAL RESEARCH

Extracellular Matrix Hydrogel Promotes Tissue Remodeling, Arteriogenesis, and Perfusion in a Rat Hindlimb Ischemia Model

Jessica L. Ungerleider, BS,[a,*] Todd D. Johnson, PhD,[a,*] Melissa J. Hernandez, BS,[a] Dean I. Elhag, BS,[a] Rebecca L. Braden, MS,[a] Monika Dzieciatkowska, PhD,[b] Kent G. Osborn, DVM, PhD,[c] Kirk C. Hansen, PhD,[b] Ehtisham Mahmud, MD,[d] Karen L. Christman, PhD[a]

VISUAL ABSTRACT

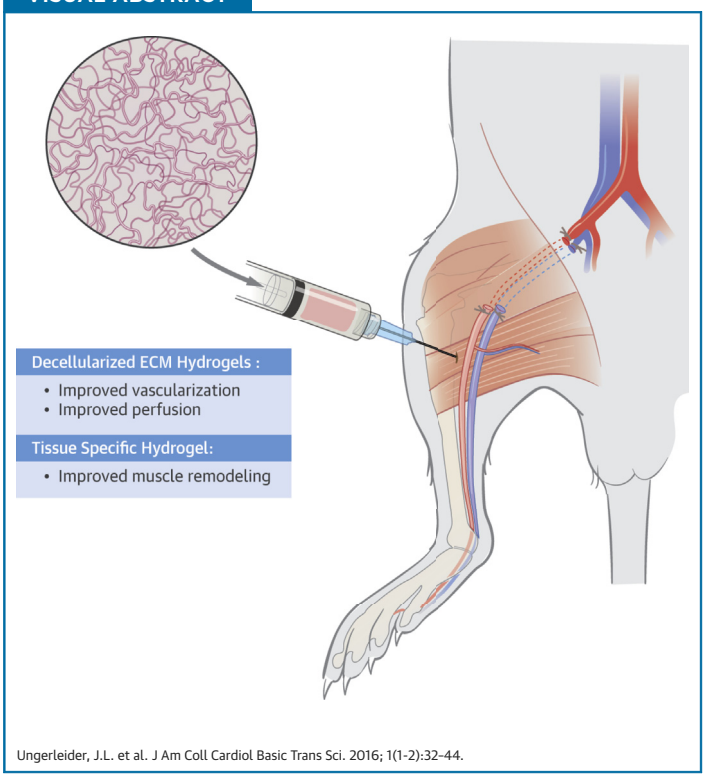

Ungerleider, J.L. et al. J Am Coll Cardiol Basic Trans Sci. 2016; 1(1-2):32-44.

HIGHLIGHTS

- **Although surgical and endovascular revascularization can be performed in patients with peripheral arterial disease (PAD), 40% of patients with critical limb ischemia do not have a revascularization option.**
- **The efficacy of an injectable tissue-specific skeletal muscle extracellular matrix (ECM) hydrogel and a human umbilical cord-derived ECM hydrogel were examined in a rodent hindlimb ischemia model.**
- **Although both biomaterials increased tissue perfusion 35 days post-injection, likely through arteriogenesis, the skeletal muscle ECM hydrogel more closely matched healthy tissue morphology.**
- **Transcriptomic analysis indicates the skeletal muscle ECM hydrogel shifted the inflammatory response, decreased necrosis/apoptosis, and increased blood vessel and muscle development.**

From the [a]Department of Bioengineering, Sanford Consortium for Regenerative Medicine, University of California San Diego, La Jolla, California; [b]Department of Biochemistry and Molecular Genetics, School of Medicine, University of Colorado, Aurora, Colorado; [c]Animal Care Program, University of California San Diego, La Jolla, California; and the [d]Division of Cardiovascular Medicine, Sulpizio Cardiovascular Center, University of California San Diego, La Jolla, California. Funding was provided in part by the National Institutes of Health (NIH) Heart, Lung, and Blood Institute (NHLBI) 5R01HL113468 (Dr. Christman), an American Heart Association Western States Innovative Sciences Award (Dr. Christman), and R33 CA183685 (Dr. Hansen). Dr. Johnson was funded by the National Science Foundation as a Graduate Student Research Fellow, the NHLBI as a Training Grant Recipient, and the Charles Lee Powell Foundation (La Jolla, California) as a Powell Fellow. Ms. Ungerleider was funded by the NIH as a Training Grant Recipient and by the San Diego Fellowship (UCSD). Dr. Christman is cofounder, board member, consultant, and holds equity interest in Ventrix, Inc.; and is an inventor on patent applications associated with this work and owned by UCSD. All other authors have reported that they have no relationships relevant to the contents of this paper to disclose. *The first 2 authors contributed equally to this work.

Manuscript received December 11, 2015; revised manuscript received January 19, 2016, accepted January 20, 2016.

SUMMARY

Although surgical and endovascular revascularization can be performed in peripheral arterial disease (PAD), 40% of patients with critical limb ischemia do not have a revascularization option. This study examines the efficacy and mechanisms of action of acellular extracellular matrix-based hydrogels as a potential novel therapy for treating PAD. We tested the efficacy of using a tissue-specific injectable hydrogel derived from decellularized porcine skeletal muscle (SKM) and compared this to a new human umbilical cord-derived matrix (hUC) hydrogel, which could have greater potential for tissue regeneration because of the younger age of the tissue source. In a rodent hindlimb ischemia model, both hydrogels were injected 1-week post-surgery and perfusion was regularly monitored with laser speckle contrast analysis to 35 days post-injection. There were significant improvements in hindlimb tissue perfusion and perfusion kinetics with both biomaterials. Histologic analysis indicated that the injected hydrogels were biocompatible, and resulted in arteriogenesis, rather than angiogenesis, as well as improved recruitment of skeletal muscle progenitors. Skeletal muscle fiber morphology analysis indicated that the muscle treated with the tissue-specific SKM hydrogel more closely matched healthy tissue morphology. Whole transcriptome analysis indicated that the SKM hydrogel caused a shift in the inflammatory response, decreased cell death, and increased blood vessel and muscle development. These results show the efficacy of an injectable ECM hydrogel alone as a potential therapy for treating patients with PAD. Our results indicate that the SKM hydrogel improved functional outcomes through stimulation of arteriogenesis and muscle progenitor cell recruitment. (J Am Coll Cardiol Basic Trans Sci 2016;1:32–44)

More than 27 million patients in North America and Europe have been diagnosed with peripheral artery disease (PAD) (1). This disease leads to an estimated 120,000 patients in the United States and 100,000 patients in Europe requiring lower extremity amputations annually due to decreased limb perfusion (2). Surgical and endovascular revascularization (3) is frequently performed, but 40% of patients with critical limb ischemia (CLI) do not have a revascularization option due to extreme tissue damage and/or diffuse atherosclerotic disease (4,5). There is also a high rate of post-revascularization amputation and therefore a need to develop new tissue salvage therapy for these patients exists (6).

Minimally invasive, injectable therapies have been investigated as a promising option for treating patients with PAD. Potential therapies that utilize cells, growth factors, or gene therapies are currently in clinical trials with the goal of increasing perfusion in the ischemic limbs (7,8). Cell therapy has however been plagued by poor cell retention and survival, as well as the viability and expense issues surrounding a living product. Growth factor therapies have suffered from poor retention of therapeutic proteins in the tissue, and gene delivery results have not translated to clinical benefit (9). While injectable biomaterial alone approaches have been explored to treat ischemic cardiac muscle (10,11), they have not been extensively explored for treating the ischemic skeletal muscle associated with PAD. When designed appropriately, injectable biomaterials can be employed to create new scaffolds that recruit endogenous cells to repair damaged tissue.

SEE PAGE 45

Our group previously developed an injectable hydrogel derived from decellularized porcine skeletal muscle extracellular matrix (SKM) (12). Preliminary histological analysis within the local region of the injected biomaterial in a mild rodent hindlimb ischemia model suggested that this acellular approach has the potential to not only stimulate vessel growth, but also could aid in treating the muscle atrophy associated with PAD (12). However, the global effect on neovascularization and muscle remodeling, as well as functional perfusion, which is a mainstay of translational studies for PAD, were not assessed. In the present study we

ABBREVIATIONS AND ACRONYMS

CLI = critical limb ischemia

ECM = extracellular matrix

hUC = human umbilical cord matrix

LASCA = laser speckle contrast analysis

PAD = peripheral artery disease

SKM = skeletal muscle matrix

FIGURE 1 Functional Perfusion Study Design in a Rat Hindlimb Ischemia Model

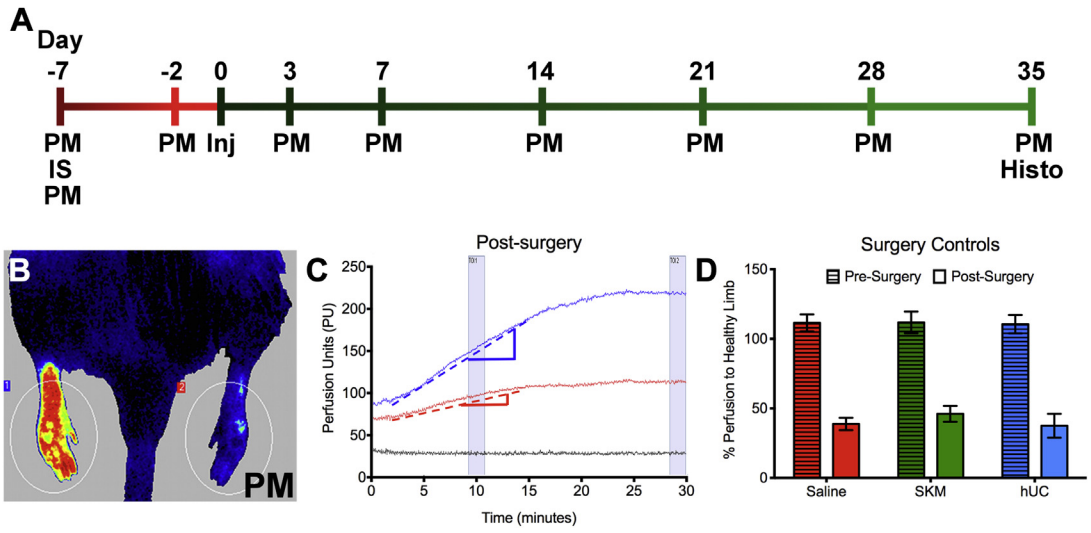

(A) In vivo study timeline. **(B)** Hindlimb perfusion measured with laser speckle contrast analysis (LASCA). Image is post-surgery with a significant decrease in perfusion of the ischemic **(right)** limb compared to the healthy **(left)** limb. **(C)** Example perfusion measurement for a single ischemic animal. Healthy limb **(blue line)**, the ischemic limb **(red line)**, and total body **(black line)** are plotted over time in arbitrary units or perfusion units. Perfusion kinetics ratio was calculated by dividing the slope of the linear region of the healthy limb **(blue dotted line)** by the slope of the linear region of the ischemic limb **(red dotted line)**. **(D)** Pre-surgery and immediately post-surgery readings for each treatment group. Histo = histology; Inj = injection; IS = ischemia surgery; PM = perfusion measurement.

investigated the tissue-specific SKM hydrogel compared to a new non-tissue-specific hydrogel derived from decellularized human umbilical cord matrix (hUC) in a rodent hindlimb ischemia model with chronically reduced perfusion to test their ability to improve hindlimb tissue perfusion, neovascularization, and muscle fiber remodeling.

MATERIALS AND METHODS

Full Methods are included in the Supplemental Appendix. These include: ECM hydrogel development and characterization, in vitro proliferation and migration, hindlimb ischemia surgery and biomaterial injection, hindlimb functional perfusion measurements, histological analysis, microarray analysis and quantitative polymerase chain reaction, and statistical analysis. All experiments in this study were performed in accordance with the guidelines established by the Institutional Animal Care and Use Committee at the University of California, San Diego, and the American Association for Accreditation of Laboratory Animal Care. Briefly, unilateral hindlimb ischemia was induced in female Sprague Dawley rats by removing a 2 cm segment of the femoral artery and vein. A biomaterial alone, SKM ($n = 9$) or hUC ($n = 10$), or saline control ($n = 11$) was injected into the gracilis muscle distal from the vessel ligation 7 days post-surgery. Ischemia was confirmed and monitored with laser speckle contrast analysis (LASCA) over 35 days post-injection. SKM alone was compared to saline at 3 and 10 days post-injection with histology and whole transcriptome analysis. Data are mean ± SEM unless otherwise noted. Significance was accepted at $p < 0.05$.

RESULTS

DECELLULARIZED TISSUES CAN BE PROCESSED INTO INJECTABLE HYDROGELS AND DIFFERENTIALLY AFFECT CELL MIGRATION AND PROLIFERATION IN VITRO. For comparison to the porcine SKM hydrogel, we developed a new non-tissue-specific injectable biomaterial from decellularized human umbilical cord tissue (hUC). Biomaterial characterization, including quantitative mass spectrometry analysis (Supplemental Figure 1, Supplemental Tables 1 to 4), and in vitro

FIGURE 2 **Hindlimb Tissue Perfusion and Perfusion Kinetics**

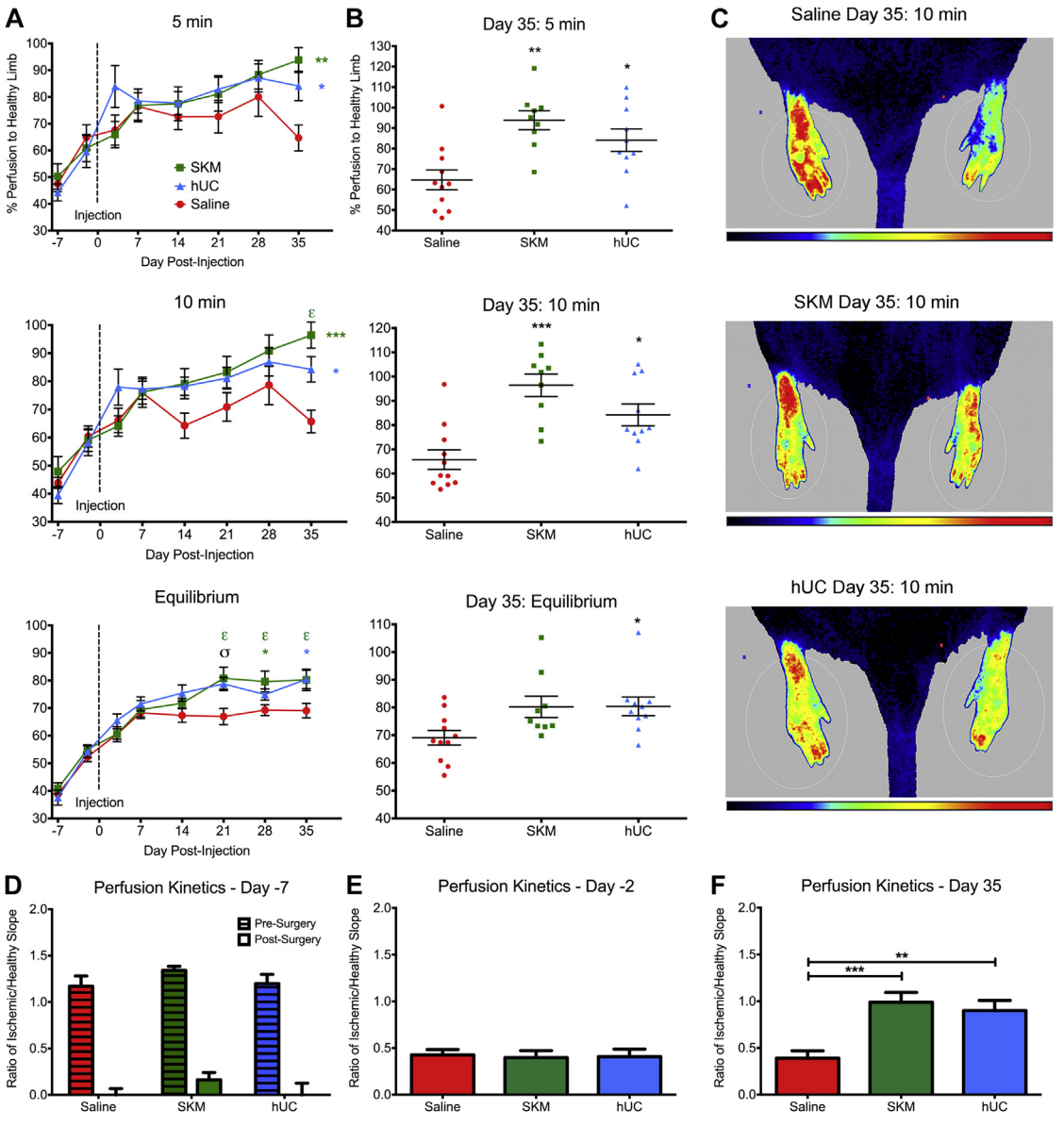

(A) Hindlimb perfusion measurements over the 42-day period for animals treated with either the skeletal muscle matrix (SKM) (n = 9), human umbilical cord matrix (hUC) (n = 10) hydrogels, or saline (n = 11). Readings are shown after the animal had been under anesthesia for 5 min, 10 min, and after reaching perfusion equilibrium. **Vertical dotted line** indicates time of treatment injection on day 0. **(B)** Individual animal perfusion readings on day 35. **(C)** Example representative perfusion images for each treatment group after the animal was under anesthesia for 10 min. Healthy limbs are on the **left** and ischemic/treated limbs are on the **right**. Note: Because the units for perfusion are arbitrary, color comparisons cannot be performed between 2 different animals. **(D)** Perfusion kinetics for pre-surgery and post-surgery. **(E)** Pre-injection perfusion kinetics on day −2 (pre-injection). **(F)** Final perfusion kinetics on day 35. A 2-way analysis of variance was conducted to compare within and between treatment groups. $\varepsilon p < 0.05$ for SKM compared to SKM at day 7 as determined by a Dunnett's multiple comparisons test. $^{*}p < 0.05$, $^{**}p < 0.01$, and $^{***}p < 0.001$, and $\sigma p < 0.05$ for both treatment groups compared to saline using a Tukey post hoc test.

FIGURE 3 Histological Assessment of Arteries and Capillaries

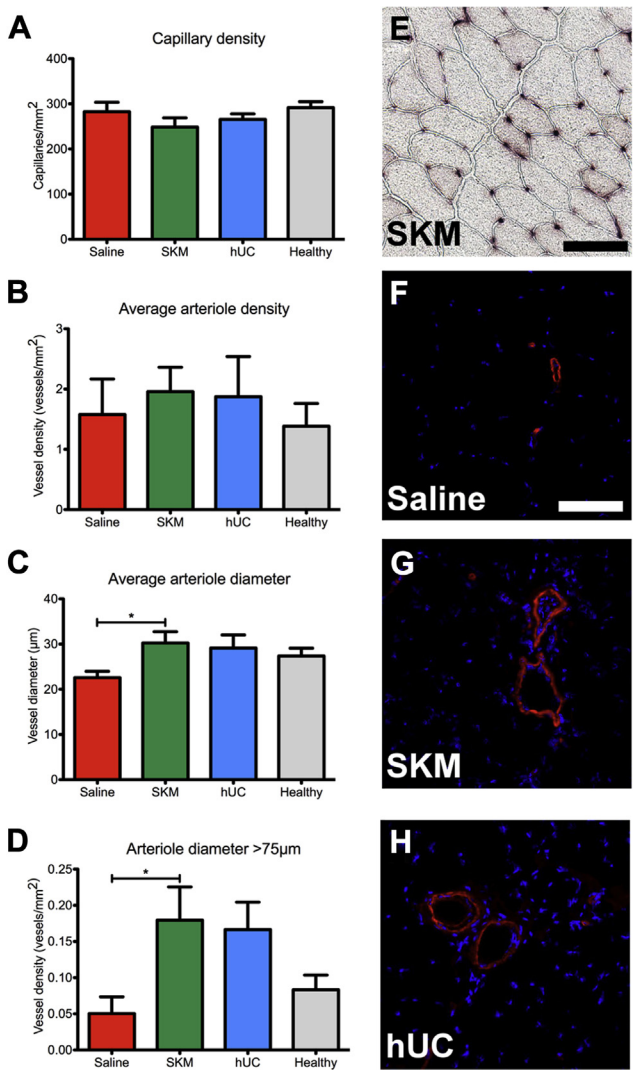

(A) Capillary density quantification. **(B)** There were no differences in arteriole density between all groups, but **(C)** the average arteriole diameter ($p = 0.0389$) and **(D)** density of arterioles with diameter >75 μm ($p = 0.0344$) was significantly increased in the skeletal muscle matrix (SKM) group. Data from the healthy limb is shown as a reference. **(E)** Representative image of capillaries stained by alkaline phosphatase for the SKM treatment group. **(F)** Example arteriole staining with anti-αSMA **(red)** and nuclei **(blue)** for saline ($n = 11$), **(G)** SKM ($n = 9$), and **(H)** human umbilical cord matrix (hUC) ($n = 10$). *$p < 0.05$ and scale bars are 100 μm.

effects on cell proliferation and migration (Supplemental Figure 2) are described in the Supplemental Appendix.

INJECTABLE ECM HYDROGELS INCREASE HINDLIMB TISSUE PERFUSION. To mimic chronically reduced perfusion associated with PAD, a rat hindlimb ischemia model was utilized (Figure 1A). ECM hydrogels or saline were injected 1 week after ischemia induction (day 0), and tissue perfusion was assessed utilizing LASCA (Figure 1B) (13). LASCA allowed for continuous monitoring and instantaneous full-field analysis of an animal with readings lasting at least 20 min to reach perfusion equilibrium (Figure 1C). Percent perfusion of the ischemic limb to healthy limb was calculated once the animal had been under anesthesia for 5 min, 10 min, and then after reaching perfusion equilibrium, to allow for comparison to currently published laser Doppler data, which is only analyzed at a single time point post-anesthesia induction, typically around 10 min (14,15). Both the pre- and immediately post-surgery perfusion measurements were compared between treatments group and shown to not be statistically different by a 2-way analysis of variance (Figure 1D).

Both of the injected hydrogels alone, SKM or hUC, led to a significant increase in percent perfusion compared to saline as early as day 21 post-injection (Figure 2A) and this improvement was maintained until the end of the study on day 35 (Figures 2B and 2C). For example, the day 35 measurements after being under anesthesia for 10 min (a typical time for laser Doppler measurements) (14) showed the ischemic damaged limb to be perfused at 65.7 ± 13.3% for saline, 96.4 ± 13.8% for SKM ($p < 0.001$, compared to saline), and 84.2 ± 14.3% for hUC ($p < 0.05$, compared to saline). All 3 perfusion assessments, at 5 and 10 min under anesthesia and at equilibrium, showed that saline animals plateaued 7 days post-injection; subsequent measurements at days 14, 21, 28, and 35 were not statistically different than at day 7 (Figure 2A) ($p > 0.05$). Animals injected with hUC hydrogel also did not significantly improve from their perfusion at day 7 (Figure 2A) ($p > 0.05$). In contrast, perfusion in SKM animals was significantly higher at day 35 compared to day 7 at the 10-min reading, and at days 21, 28, and 35 compared to day 7 at equilibrium (Figure 2A) ($p < 0.05$).

Due to the use of LASCA we were able to monitor dynamic perfusion while the animals were under anesthesia. The animals were initially anesthetized with 5% isoflurane and then transferred to 2.5% when the perfusion reading started. Decreasing the level of isoflurane creates an increase in cardiac output and blood perfusion in the peripheral skeletal muscle (16). Thus, the perfusion increased in the hindlimbs as the animal rested on the deck, as illustrated in Figure 1C. From this data, a new

FIGURE 4 Biocompatibility Assessment and Muscle Fiber Morphology Quantification

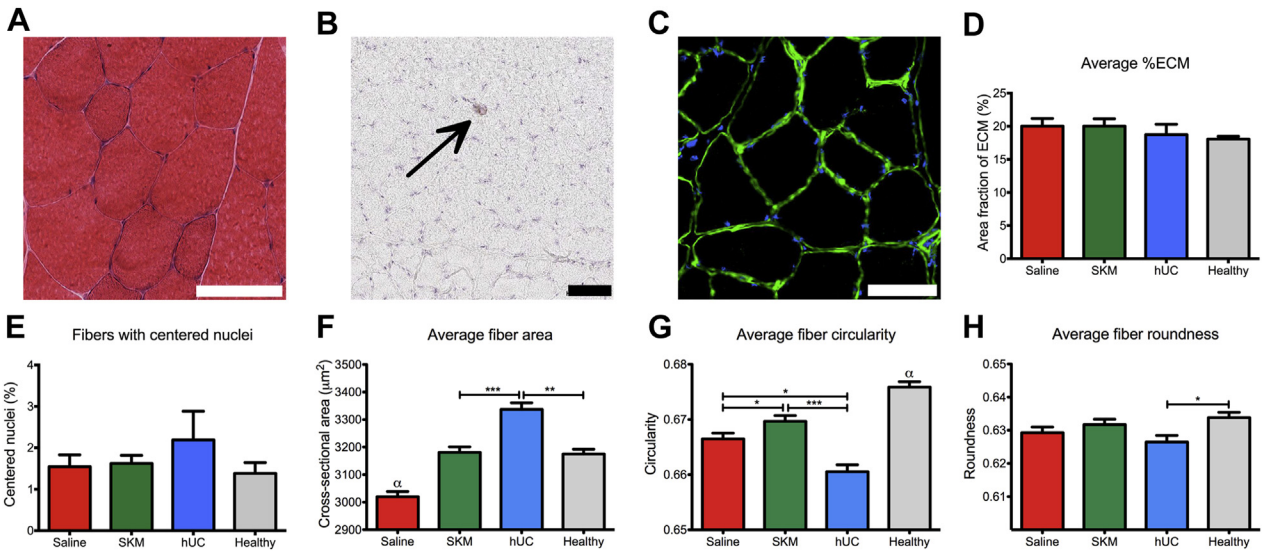

(A) Hematoxylin and eosin (H&E) stained transverse section showing healthy fiber morphology. **(B)** Macrophages were stained with CD68 as shown **(black arrow)**. **(C)** Extracellular matrix stained with a laminin antibody **(green)** and nuclei were counter stained **(blue)** for saline (n = 11), human umbilical cord matrix (hUC) (n = 10), and skeletal muscle matrix (SKM) (n = 9) treated animals. **(D)** Percent ECM was measured from laminin stained slides. **(E)** Percent of fibers with centrally located nuclei. **(F)** Average fiber area. **(G)** Average fiber circularity. **(H)** Average fiber roundness. Scale bars are 100 μm and all images are representative from an SKM hydrogel treated animal. *$p < 0.05$, **$p < 0.01$, ***$p < 0.001$, and α$p < 0.001$ compared to all other groups.

parameter called perfusion kinetics ratio can be reported to show the rate of change of perfusion over time. This was calculated as a ratio of the slopes from the linear region of the perfusion measurements (indicated by dotted lines on Figure 1C) from the ischemic foot to the healthy foot. Perfusion kinetics ratios that deviate from 1 thus illustrate differences in perfusion between the 2 legs, with values <1 demonstrating a slower response to changes in cardiac output in the ischemic limb. The healthy animals pre-surgery had symmetric perfusion rates in each limb, or a perfusion kinetics ratio near 1 (Figure 2D). Immediately post-surgery, the ischemic damaged tissue showed a decreased rate of change in perfusion, which is indicated by the perfusion kinetics ratio being close to zero for all groups (Figure 2D). By day 5 post-ischemia (2 days pre-injection), the animals had partially recovered due to endogenous healing mechanisms and produced consistently improved perfusion kinetics ratios of approximately 0.4 (Figure 2E). Finally, by the end of the study, perfusion kinetics ratios for the SKM and hUC hydrogels showed significant improvements over the saline ($p < 0.001$ for SKM; $p < 0.01$ for hUC) control, which was maintained at approximately 0.4 (Figure 2F).

ECM HYDROGELS STIMULATED INCREASED DENSITY OF LARGER ARTERIOLES. Capillary and arteriole densities were analyzed on tissue cross-sections sampled throughout the entire gracilis muscle at day 35. Although average capillary (Figure 3A) and arteriole density (Figure 3B) did not vary between treatment groups, there was a significant increase in the average arteriole diameter for SKM animals compared to saline (Figure 3C). More specifically there was an increase in the density of larger arterioles with a diameter >75 μm (Figure 3D). Similar trends were observed for the hUC hydrogel, but were not statistically significant compared to saline. A representative image of capillary staining for the SKM group is shown in Figure 3E, while example arteriole staining from all treatment groups is shown in Figures 3F to 3H.

HYDROGELS WERE FULLY DEGRADED WITHOUT A CHRONIC INFLAMMATORY RESPONSE AND SKM HYDROGEL PROMOTES MUSCLE REMODELING. On

FIGURE 5 Short-Term Histological Assessment of Arteries and Capillaries

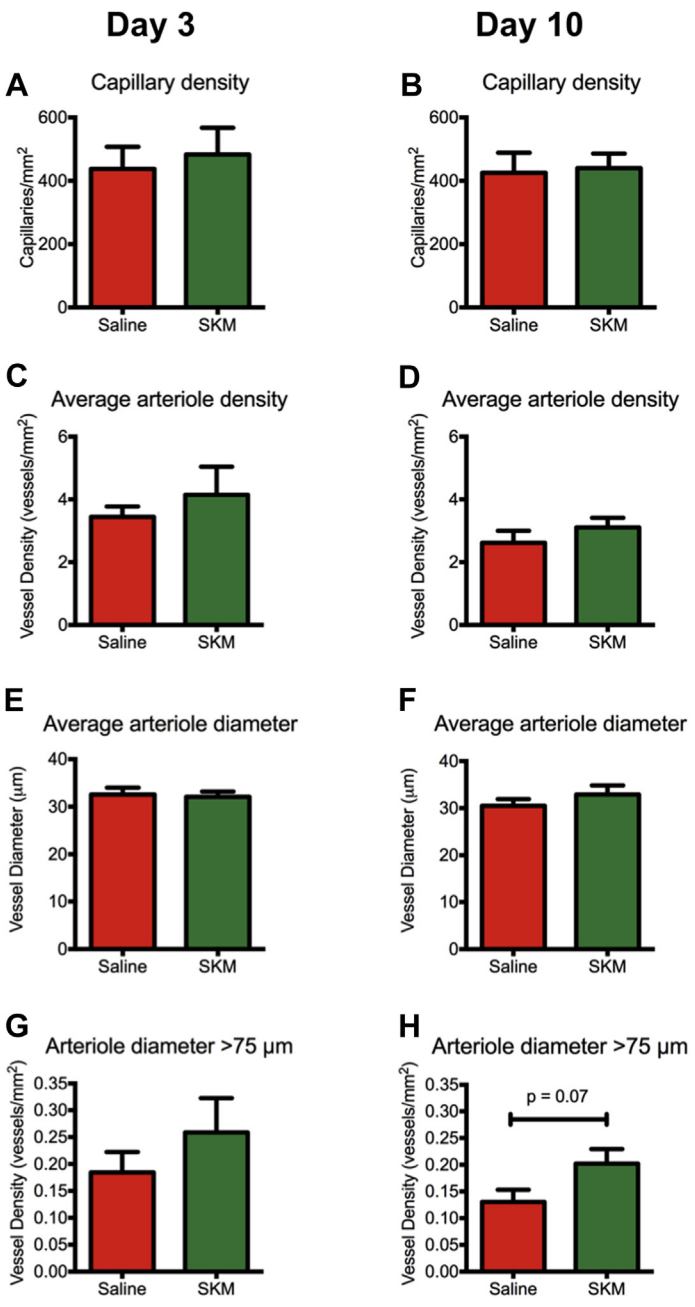

Histological analysis taken at **(A, C, E, G)** day 3 and **(B, D, F, H)** day 10 post-injection. There were no differences in **(A, B)** capillary density, **(C, D)** arteriole density, or **(E, F)** average arteriole diameter between SKM and saline at these early timepoints, but **(E,F)** the density of arterioles with diameter >75 μm trended higher in the SKM (n = 6) group compared to saline (n = 6).

day 35 post-injection, hindlimb muscle tissue cross sections were stained with hematoxylin and eosin and analyzed by a histopathologist blinded to the treatment groups. Histological analysis concluded that the biomaterials had fully degraded, and no scarring or chronic inflammatory response was observed. Macrophages in the tissue were very low in density, seen as only single cells evenly spaced throughout the tissue. Representative images from the SKM group are shown in Figures 4A and 4B. Next, laminin staining (Figure 4C) was utilized to measure area fraction of ECM to assess interstitial ECM deposition (17). No significant differences were observed with about 20% of the surveyed area being covered by positively stained laminin (Figure 4D).

Fibers with centrally located nuclei can be an indicator of abnormal fibers, representing damaged or remodeling muscle (18). No significant differences in the percentage of fibers with centrally located nuclei were observed by day 35, with an average of about 2% of the fibers (Figure 4E). Individual fiber morphology (cross-sectional area, circularity, and roundness) was also measured and the batched quantified fiber populations were analyzed for animals treated with saline (7,946 fibers), SKM hydrogel (8,302 fibers), and hUC hydrogel (6,000 fibers) compared to healthy tissue (9,130 fibers). The average fiber area of SKM hydrogel-treated animals was not significantly different than the healthy tissue (Figure 4F). In contrast, the average fiber area of the hUC hydrogel group was significantly higher than the SKM hydrogel ($p < 0.001$) and healthy tissue ($p < 0.01$), and saline was significantly less than all groups ($p < 0.001$) (Figure 4F). Next, fiber circularity (ratio of short axis to long axis) and fiber roundness (roughness or angularity) of the muscle fibers also showed SKM was most similar to the healthy tissue (Figures 4G and 4H).

SKM HYDROGEL IMPROVED PERFUSION AND MUSCLE REMODELING THROUGH INCREASED DENSITY OF LARGER ARTERIOLES AND RECRUITMENT OF SKELETAL MUSCLE PROGENITORS. We next sought to analyze the temporal changes following ECM hydrogel injection. We chose to focus subsequent studies on the tissue-specific SKM hydrogel as it had improved muscle remodeling compared to the hUC hydrogel and because its readily available tissue sourcing would make it cheaper and easier to manufacture as a clinical product. We performed an additional hindlimb ischemia study, comparing saline and SKM injections at 3 and 10 days

FIGURE 6 Short-Term Histological Assessment of Skeletal Muscle Progenitor Cells

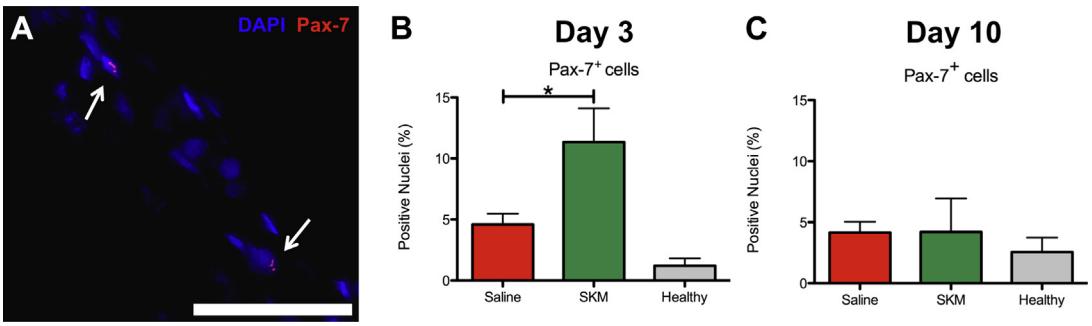

(A) Representative image of Pax-7$^+$ **(red)** and Hoechst 33342 **(blue)** costaining in skeletal muscle matrix (SKM)–injected gracilis muscle. Scale bar is 50 μm and Pax-7$^+$ nuclei are indicated by **white arrows**. There were significantly more Pax-7$^+$ cells as a percentage of total nuclei in SKM ($n = 6$) versus saline ($n = 6$) injected muscles at **(B)** day 3, but this returned to quiescent levels by **(C)** day 10. *$p = 0.0096$. Data from the healthy limb is shown as a reference.

post-injection (day 10 and day 17 post-surgery, respectively). There were no significant differences in capillary density, arteriole density, or arteriole diameter between saline and SKM treated muscles at these early time points (**Figures 5A to 5F**). However, similar to the previous experiment at day 35, density of arterioles >75 mm trended higher in SKM injected animals at both 3 and 10 days post-injection (**Figures 5G and 5H**).

Due to improvements in muscle remodeling at day 35 post-injection, we analyzed tissue at day 3 and 10 post-injection for infiltration of skeletal muscle progenitors. Pax-7 is a transcription factor involved in early stage muscle lineage commitment in skeletal muscle satellite cells (19). Analysis of percentage of Pax-7 positive nuclei (**Figure 6A**) showed the impact of SKM injection on the gracilis muscle near the material. At day 3, SKM injected muscles had a significantly higher percentage of Pax-7$^+$ nuclei compared to saline (**Figure 6B**) ($p < 0.05$), but by day 10 Pax-7$^+$ nuclei dropped to more quiescent levels (**Figure 6C**).

SKM HYDROGEL PROMOTES A PRO-REGENERATIVE ENVIRONMENT. We further investigated the mechanism of action of the SKM hydrogel through whole transcript array analysis. Using a false discovery rate of $q < 0.1$, there were 561 significantly differentially regulated genes between saline and SKM in the gracilis at 3 days and 16 genes at 10 days (Supplemental Table 5). At 3 days post-injection, Ingenuity pathway analysis showed shifts in the inflammatory response and lipid and carbohydrate metabolism, and increases in muscle development and cell survival with SKM (**Table 1**). Furthermore, there was down-regulation of genes related to cell death, response to hypoxia, ECM and cytoskeletal organization, and blood vessel development. At 10 days post-injection, there continued to be a shift in the inflammatory response and down-regulation of cell death as well as up-regulation of cell adhesion and motility, ECM organization, blood vessel development, and neural system development pathways. Gene ontology analysis also showed differences in many molecular functions and biological processes, such as binding (GO:0005488), catalytic activity (GO:0003824), metabolic process (GO:0008152), developmental process (GO:0032502), and immune system process (GO:0002376), between groups at both time points (Supplemental Figures 6 to 9). Microarray analysis was validated with quantitative polymerase chain reaction of key genes (Supplemental Figure 3, Supplemental Table 10).

DISCUSSION

Various neovascularization therapeutic approaches including cells, growth factors, and gene therapies have been explored, but have been met with mixed results in clinical trials for treating patients with CLI associated with PAD (20). A biomaterial only therapeutic approach could have several advantages compared to the existing paradigm including off-the-shelf availability, reduced cost, and the ability to

TABLE 1 Significantly Altered Pathways in SKM Relative to Saline Injected Muscle at 3 and 10 Days Post-Injection, as Determined by Ingenuity Pathway Analysis

Category	Annotation	p Value	*z*-score	# Molecules
Day 3 up-regulated pathways				
Lipid metabolism, small molecule biochemistry	Conversion of lipid	0.0112	1.387	5
Cellular development, cellular growth and proliferation, hematological system development and function	Proliferation of lymphocytes	0.0027	1.381	9
Cell death and survival	Cell survival	0.0272	0.96	21
Cellular compromise, inflammatory response	Degranulation of leukocyte cell lines	<0.001	0.748	8
Cell morphology, cellular function and maintenance	Transmembrane potential of mitochondria	0.0021	0.706	9
Cell signaling, molecular transport, vitamin and mineral metabolism	Quantity of Ca2+	0.0396	0.699	16
Carbohydrate metabolism	Uptake of monosaccharide	0.0233	0.653	8
Cellular function and maintenance	Endocytosis	0.0075	0.555	11
Cellular development, cellular growth and proliferation, organ development, skeletal and muscular system development and function, tissue development	Proliferation of muscle cells	<0.001	0.486	22
Cell morphology, skeletal and muscular system development and function	Contractility of muscle cells	0.0115	0.305	4
Day 3 down-regulated pathways				
Cell-to-cell signaling and interaction	Activation of cells	0.0161	-2.919	15
Cell death and survival	Necrosis	0.0139	-2.126	58
Cell signaling, post-translational modification	Tyrosine phosphorylation of protein	0.0401	-2	4
Cell death and survival	Neuronal cell death	0.0011	-1.949	36
Cardiovascular system development and function, organismal development	Vasculogenesis	0.0029	-1.604	15
Cell death and survival	Apoptosis	<0.0001	-1.484	75
Cellular movement	Cell movement	<0.001	-1.39	43
Cell Signaling, molecular transport, small molecule biochemistry, vitamin and mineral metabolism	Release of Ca2+	0.0486	-1.154	6
Cardiovascular system development and function, organismal development	Angiogenesis	0.0050	-1.107	19
Cellular assembly and organization, cellular function and maintenance	Organization of cytoskeleton	0.0127	-0.905	45
Day 10 up-regulated pathways				
Cellular movement	Cell movement	0.0089	1.709	7
Cellular movement	Migration of cells	0.0453	1.455	5
Cardiovascular system development and function, organismal development	Vasculogenesis	0.0037	1	4
Cellular growth and proliferation	Proliferation of cells	<0.00001	0.986	20
Inflammatory response	Inflammatory response	0.0125	0.447	5
Cell morphology, cellular assembly and organization, cellular development, cellular growth and proliferation, nervous system development and function, tissue development	Outgrowth of neurites	<0.001	0.447	6
Cardiovascular system development and function, organismal development	Angiogenesis	0.0023	0.277	5
Day 10 down-regulated pathways				
Cell death and survival	Cell death	<0.001	-0.977	15
Cell death and survival	Apoptosis	0.0050	-0.594	11

stimulate endogenous cell recruitment over multiple days or weeks. In this study, we demonstrate the first functional analysis of an injectable ECM-based hydrogel for treating PAD by showing increased perfusion in a hindlimb ischemia model and evidence for improvement of the underlying muscle pathology. We also present one of the first studies to investigate the mechanisms of action behind decellularized injectable hydrogels through an unbiased whole transcriptome analysis.

In this study, we used a newer imaging modality, LASCA, to assess perfusion in the feet, which allowed for instantaneous and continuous monitoring of the perfusion in the limbs. This provided insight into the change in perfusion over time. For comparison to previous publications that used laser

Doppler technology, which can only take a static snapshot at a given time point (14,15), typically within 10 min, we reported perfusion measurements at 3 distinct time intervals after the onset of anesthesia. At all 3 readings, the ECM hydrogels significantly increased perfusion over the saline control. In analyzing the equilibrium measurements, which showed the least animal-to-animal variability, perfusion increased over 3 weeks and plateaued at day 21, which corresponds with the material degradation time of approximately 3 weeks (12). The increases persisted out to day 35 post-injection. By using LASCA, we were also able to characterize the dynamic perfusion changes under anesthesia through calculation of the perfusion kinetics ratio. This new measurement provides insight into the health of the vascular network and its ability to transition through a change in cardiac output. By day 35, only the biomaterial treated groups had perfusion kinetics ratios return to 1, indicating the vessel network in the ischemic limb was able to respond to changes in cardiac output at the same rate as the healthy limb. This is clinically relevant because patients with PAD and CLI have shown a decreased or slowed rate of perfusion in transition from states of lower perfusion to higher perfusion. The decreased rate of change of perfusion is associated with decreased vessel health and compliance in diseased patients (21,22). The increase in perfusion and restoration of hindlimb perfusion kinetics directly correlated with histological quantification, which showed an increased density of arterioles with diameters >75 μm throughout the whole muscle, suggesting that the biomaterial therapy acts via promoting arteriogenesis rather than angiogenesis because capillary density was not increased at any of the investigated time points. Other studies have indicated that a therapy impacting arteriogenesis rather than angiogenesis may be more desirable for CLI patients (23,24).

While several in vitro studies have shown the importance of ECM tissue specificity (25–29), limited studies have examined whether tissue specificity is necessary in vivo. In this study, we tested 2 different ECM-derived hydrogels, which were both biocompatible. The SKM hydrogel represents a tissue-specific ECM approach for treating skeletal muscle. For comparison, a new injectable hydrogel derived from human umbilical cords was developed as a non-tissue-specific approach and as an ECM source with potential for increased regeneration due to its young age. In vitro, we show differences in the 2 tissue sources with respect to their effects on cell proliferation and migration, but in vivo, while some perfusion measures showed trends toward an increase with SKM, both materials were capable of significantly enhancing perfusion over the saline control. Decellularized ECMs, including those from xenogeneic sources and those processed into hydrogels, have been shown to promote tissue remodeling and healing in a variety of applications (12,30–32). This positive tissue remodeling has been attributed to a shift toward a pro-remodeling immune response associated with Th2 lymphocytes and M2 macrophages (33,34). Since we observed an increase in perfusion with both materials this could have been caused by this shift toward a more pro-remodeling vs. pro-inflammatory response, and suggests that non-tissue-specific responses such as vascularization may be possible with non-tissue-specific ECM. However, when we examined measures of skeletal muscle remodeling post-ischemic injury, we found that the SKM hydrogel treated animals most closely matched the morphology of healthy skeletal muscle and were significantly different than the hUC hydrogel treated animals. While the 2 ECM hydrogels are derived from different species, they are both xenogeneic in this model. In addition, given the different gelation characteristics, there are likely small differences in the mechanical properties between the 2 gels. However, several studies have shown tissue-specific responses with decellularized ECM in vitro (25–28), many of which used 2D coatings where only the biochemical cues and not the mechanical properties were different. Taken together with our in vivo results, this suggests that tissue specificity of the material may be important for overall tissue remodeling and regeneration. We show through a targeted ECM proteomics approach that SKM and hUC do have distinct ECM component signatures despite being predominantly composed of collagen I. This may be important for muscle regeneration, given evidence in the literature correlating differential ECM composition with human myoblast proliferation (35). When we examined the ischemic muscle shortly after injection of the SKM hydrogel, we found an increase in Pax-7^{+} skeletal muscle progenitor cells. Pax-7 is up-regulated in regenerating muscle, but usually is expressed in about 5% of nuclei in quiescent muscle (19). This suggests that the SKM hydrogel is causing early stimulation of muscle regeneration through recruitment of satellite cells within the first week of material injection, which may have resulted in the improved measures

JACC: BASIC TO TRANSLATIONAL SCIENCE VOL. 1, NO. 1-2, 2016
JANUARY/FEBRUARY 2016:32–44

of muscle health we observed at 35 days post-injection.

Due to the improvements in muscle remodeling, as well as the improved translational outlook of SKM over hUC because of the ease, cost, and reduced variability with a porcine tissue source, we chose to further investigate dynamic changes in the global transcriptome due to SKM hydrogel injection. Although microarray analysis has previously been employed to characterize the preclinical hindlimb ischemia model (36,37) and human PAD patients (38), no studies have investigated the effect of therapeutic interventions using this global unbiased analysis. At day 3, comparisons between SKM and saline controls showed that the SKM hydrogel promoted cell survival pathways, immune response, and muscle proliferation and contractility, while at day 10 the up-regulated pathways shifted emphasis to vascular development, neuron outgrowth, and cell motility. Genes associated with extracellular matrix (ECM) were down-regulated at day 3 but became up-regulated at day 10. This correlates with other studies of transcriptomic effects of skeletal muscle regeneration, which show that ECM being up-regulated at later time points is associated with tissue repair, cell migration, and myogenic development (39). Interestingly, apoptosis and response to hypoxia were strongly down-regulated at both time points, suggesting a pro-survival and regenerative response of the SKM material compared to the saline control across the entire muscle. These results suggest that the SKM hydrogel produces functional outcomes through altering key pathways associated with inflammatory response, cell death and survival, metabolism, and vessel and muscle development.

STUDY LIMITATIONS. Limitations of this study are due to the inherent weaknesses of hindlimb ischemia preclinical models for modeling PAD and CLI. Unfortunately, no preclinical model fully mimics all aspects of PAD or CLI. In particular, all hindlimb ischemia models are acute models, while PAD is a chronic condition (40). The standard models for PAD and CLI are rodent models, which due to young age and healthy collateral architecture often heal to a great extent without any therapeutic interventions (40,41). Even large animal models and other rodent models that mimic aspects of the patient population, such as hyperhomocysteinemia, diabetes, hypercholesterolemia, and/or aging, still show collateral vessel formation (40). To partially address these limitations, we selected a vessel ligation and excision protocol, which resulted in chronically reduced perfusion (~65%) and muscle atrophy (reduced muscle fiber cross-sectional area). While our model did not have accompanying necrosis of the toes or feet, it permitted us to inject the biomaterials 7 days post-ischemic injury to allow the acute response from the surgery to resolve prior to treatment. The small scale is another limitation of these animal models. Here we delivered a single bolus into the ischemic damaged region, whereas in human patients multiple injections would be utilized.

CONCLUSIONS

We have shown the efficacy of an injectable biomaterial alone (SKM or hUC) to increase tissue perfusion in a rat hindlimb ischemia study. Significant differences in muscle remodeling at a chronic time point indicate that utilizing a tissue-specific biomaterial therapy for PAD may be more desirable. Furthermore, improved arteriogenesis and skeletal muscle progenitor cell recruitment at shorter time points and gene expression differences related to inflammatory response, blood vessel and muscle tissue development, apoptosis, cell survival, and metabolism give evidence of a transcriptome-wide improvement in tissue regeneration due to the SKM hydrogel.

ACKNOWLEDGMENTS The authors would like to thank Carolina Rodgers and Sandra Leon-Garcia (supervised by Dr. Louise Laurent) for their help with harvesting tissue samples, Matt Joens from the Waitt Advanced Biophotonics Center at the Salk Institute for his expertise with SEM, and Jorge Valencia and Stacey Huynh from the Veterans Association and the Veterans Medical Research Foundation Microarray and Next Generation Sequencing Core at the University of California, San Diego, for their expertise with Affymetrix microarrays.

REPRINT REQUESTS AND CORRESPONDENCE: Dr. Karen L. Christman, Department of Bioengineering, Sanford Consortium for Regenerative Medicine, University of California San Diego, 2880 Torrey Pines Scenic Drive, La Jolla, California 92037. E-mail: christman@eng.ucsd.edu.

PERSPECTIVES

COMPENTENCY IN MEDICAL KNOWLEDGE: In a rat model, injection of naturally derived ECM hydrogels improved perfusion to the ischemic hindlimb. This is the first pre-clinical study to specifically investigate the effect of ECM hydrogels on functional perfusion in hindlimb ischemia models.

TRANSLATIONAL OUTLOOK 1: Satisfaction of current Good Manufacturing Practice regulations and additional toxicology studies will be required prior to translation; however, this functional study combined with the current clinical use of porcine derived decellularized ECM and initiation of a clinical trial with a similar cardiac ECM derived hydrogel (NCT02305602) provides support for the advancement of the SKM hydrogel into clinical trials for treating patients with advanced PAD.

TRANSLATIONAL OUTLOOK 2: Considering this was a small animal study with a single bolus injection, the optimal number of injection sites and site locations would need to be optimized for human patients. Also, the potential exists for injecting a patient with the therapy several times over numerous months, which was not explored here.

REFERENCES

1. Hirsch AT, Haskal ZJ, Hertzer NR, et al. ACC/AHA 2005 Practice Guidelines for the management of patients with peripheral arterial disease (lower extremity, renal, mesenteric, and abdominal aortic). Circulation 2006;113:e463–654.

2. Lawall H, Bramlage P, Amann B. Stem cell and progenitor cell therapy in peripheral artery disease. A critical appraisal. Thromb Haemost 2010; 103:696–709.

3. Adam DJ, Beard JD, Cleveland T, et al. Bypass versus angioplasty in severe ischaemia of the leg (BASIL): multicentre, randomised controlled trial. Lancet 2005;366:1925–34.

4. Dormandy J, Heeck L, Vig S. The fate of patients with critical leg ischemia. Semin Vasc Surg 1999; 12:142–7.

5. Marston WA, Davies SW, Armstrong B, et al. Natural history of limbs with arterial insufficiency and chronic ulceration treated without revascularization. J Vasc Surg 2006;44: 108–14.

6. Isner JM, Rosenfield K. Redefining the treatment of peripheral artery disease: role of percutaneous revascularization. Circulation 1993;88: 1534–57.

7. Raval Z, Losordo DW. Cell therapy of peripheral arterial disease: from experimental findings to clinical trials. Circ Res 2013;112:1288–302.

8. Powell RJ. Update on clinical trials evaluating the effect of biologic therapy in patients with critical limb ischemia. J Vasc Surg 2012;56: 264–6.

9. Gupta R, Tongers J, Losordo DW. Human studies of angiogenic gene therapy. Circ Res 2009;105:724–36.

10. Rane AA, Christman KL. Biomaterials for the treatment of myocardial infarction: a 5-year update. J Am Coll Cardiol 2011;58:2615–29.

11. Tous E, Purcell B, Ifkovits JL, Burdick JA. Injectable acellular hydrogels for cardiac repair. J Cardiovasc Transl Res 2011;4:528–42.

12. Dequach JA, Lin JE, Cam C, et al. Injectable skeletal muscle matrix hydrogel promotes neovascularization and muscle cell infiltration in a hindlimb ischemia model. Eur Cell Mater 2012;23: 400–12.

13. Senarathna J, Rege A, Li N, Thakor NV. Laser speckle contrast imaging: theory, instrumentation and applications. IEEE Rev Biomed Eng 2013;6: 99–110.

14. Niiyama H, Huang NF, Rollins MD, Cooke JP. Murine model of hindlimb ischemia. J Vis Exp 2009;23:1035.

15. Limbourg A, Korff T, Napp LC, Schaper W, Drexler H, Limbourg FP. Evaluation of postnatal arteriogenesis and angiogenesis in a mouse model of hind-limb ischemia. Nat Protoc 2009;4:1737–46.

16. Hartman JC, Pagel PS, Proctor LT, Kampine JP, Schmeling WT, Warltier DC. Influence of desflurane, isoflurane and halothane on regional tissue perfusion in dogs. Can J Anaesth 1992;39:877–87.

17. Meyer GA, Lieber RL. Skeletal muscle fibrosis develops in response to desmin deletion. Am J Physiol Cell Physiol 2012;302:C1609–20.

18. Wróblewski R, Edström L, Mair WG. Five different types of centrally nucleated muscle fibres in man: elemental composition and morphological criteria. A study of myopathies, fetal tissue and muscle spindle. J Submicrosc Cytol 1982;14: 377–87.

19. Seale P, Sabourin LA, Girgis-Gabardo A, Mansouri A, Gruss P, Rudnicki MA. Pax7 is required for the specification of myogenic satellite cells. Cell 2000;102:777–86.

20. Ouma GO, Zafrir B, Mohler ER, Flugelman MY. Therapeutic angiogenesis in critical limb ischemia. Angiology 2013;64:466–80.

21. Haas TL, Lloyd PG, Yang HT, Terjung RL. Exercise training and peripheral arterial disease. Compr Physiol 2012;2:2933–3017.

22. Mullen MJ, Kharbanda RK, Cross J, et al. Heterogenous nature of flow-mediated dilatation in human conduit arteries in vivo: relevance to endothelial dysfunction in hypercholesterolemia. Circ Res 2001;88:145–51.

23. Buschmann I, Schaper W. Arteriogenesis versus angiogenesis: two mechanisms of vessel growth. News Physiol Sci 1999;14:121–5.

24. Scholz D, Ziegelhoeffer T, Helisch A, et al. Contribution of arteriogenesis and angiogenesis to postocclusive hindlimb perfusion in mice. J Mol Cell Cardiol 2002;34:775–87.

25. DeQuach JA, Mezzano V, Miglani A, et al. Simple and high yielding method for preparing tissue specific extracellular matrix coatings for cell culture. PloS One 2010;5:e13039.

26. French KM, Boopathy AV, DeQuach JA, et al. A naturally derived cardiac extracellular matrix enhances cardiac progenitor cell behavior in vitro. Acta Biomater 2012;8:4357–64.

27. Sellaro TL, Ravindra AK, Stolz DB, Badylak SF. Maintenance of hepatic sinusoidal endothelial cell phenotype in vitro using organ-specific extracellular matrix scaffolds. Tissue Eng 2007;13: 2301–10.

28. Cheng N-C, Estes BT, Awad HA, Guilak F. Chondrogenic differentiation of adipose-derived adult stem cells by a porous scaffold derived from native articular cartilage extracellular matrix. Tissue Eng Part A 2009;15:231–41.

29. Medberry CJ, Crapo PM, Siu BF, et al. Hydrogels derived from central nervous system extracellular matrix. Biomaterials 2013;34: 1033–40.

30. Seif-Naraghi SB, Singelyn JM, Salvatore MA, et al. Safety and efficacy of an injectable extracellular matrix hydrogel for treating myocardial infarction. Science Transl Med 2013;5:173ra25.

31. Sicari BM, Rubin JP, Dearth CL, et al. An acellular biologic scaffold promotes skeletal muscle formation in mice and humans with volumetric muscle loss. Science Transl Med 2014;6:234ra58.

32. Badylak S, Vorp D, Spievack A, et al. Esophageal reconstruction with ECM and muscle tissue in a dog model. J Surg Res 2005;128:87–97.

33. Allman A, McPherson T, Badylak S, et al. Xenogeneic extracellular matrix grafts elicit a Th2-restricted immune response. Transplantation 2001;71:1631–40.

34. Brown BN, Londono R, Tottey S, et al. Macrophage phenotype as a predictor of constructive remodeling following the implantation of biologically derived surgical mesh materials. Acta Biomater 2012;8:978–87.

35. Ferreira MM, Dewi RE, Heilshorn SC. Microfluidic analysis of extracellular matrix-bFGF crosstalk on primary human myoblast chemoproliferation, chemokinesis, and chemotaxis. Integr Biol 2015;7:569–79.

36. Paoni NF, Peale F, Wang F, et al. Time course of skeletal muscle repair and gene expression following acute hind limb ischemia in mice. Physiol Genomics 2002;11:263–72.

37. Lee CW, Stabile E, Kinnaird T, et al. Temporal patterns of gene expression after acute hindlimb ischemia in mice: insights into the genomic program for collateral vessel development. J Am Coll Cardiol 2004;43:474–82.

38. Tuomisto TT, Rissanen TT, Vajanto I, Korkeela A, Rutanen J, Yla-Herttuala S. HIF-VEGF-VEGFR-2, TNF-alpha and IGF pathways are upregulated in critical human skeletal muscle ischemia as studied with DNA array. Atherosclerosis 2004;174:111–20.

39. Goetsch SC, Hawke TJ, Gallardo TD, Richardson JA, Garry DJ. Transcriptional profiling and regulation of the extracellular matrix during muscle regeneration. Physiol Genomics 2003;14:261–71.

40. Waters RE, Terjung RL, Peters KG, Annex BH. Preclinical models of human peripheral arterial occlusive disease: implications for investigation of therapeutic agents. J Appl Physiol 2004;97:773–80.

41. Landazuri N, Joseph G, Guldberg RE, Taylor WR. Growth and regression of vasculature in healthy and diabetic mice after hindlimb ischemia. Am J Physiol Regul Integr Comp Physiol 2012;202:R48–56.

KEY WORDS biomaterial, critical limb ischemia, decellularization, hydrogel, injectable, peripheral artery disease

APPENDIX For expanded Methods, Results, and References sections as well as supplemental figures and tables, please see the supplemental appendix.